Absorption of far-infrared radiation by random metal particle composites

N. E. Russell, J. C. Garland, and D. B. Tanner
Department of Physics, The Ohio State University, Columbus, Ohio 43210

(Received 23 June 1980)

Measurements have been made of the absorption of far-infrared radiation by Pd small particles randomly embedded in KCl. The small particle specimens had Pd volume fractions between 0.001 and 0.1. At volume fractions of 0.03 and below, the absorption coefficient was proportional to the Pd concentration. The frequency dependence of the absorption coefficient was typically quadratic below 30 cm^{-1} with a slower dependence above 30 cm^{-1}. The absorption coefficients were about a factor of 10 larger than those calculated from a theory based on electric and magnetic dipole absorption.

I. INTRODUCTION

In this paper we describe far-infrared measurements on a model small-particle composite material and compare the results of these measurements with calculations. Our samples consisted of $\sim$1-μm-radius Pd particles randomly embedded in KCl at low concentration. These samples differed from those studied previously by Tanner, Sievers, and Buhrman[1] and by Granqvist, Buhrman, Wyns, and Sievers[2] in two significant ways. First, the particles used in the previous investigations had radii of $\sim$ 100 Å while our particles are a factor of 100 larger. (In very small particles, size quantization of the electron energies should cause the dielectric function of the particle to differ from that of bulk material,[3] while in larger particles the bulk dielectric function should give a good description of the properties of the particle.) Second, the earlier studies were done on unsupported powder of the small particles; no insulating matrix was used so that every particle was in contact with at least one other particle in the powder. In our samples the particles are supported by the KCl host. A preliminary account of our work has appeared elsewhere.[4]

The proper theoretical description of randomly inhomogeneous materials has been the subject of considerable discussion in recent years, both because of the intrinsic interest of random noncrystalline systems and also because of possible technological applications of these materials.[5] Three lengths characterize the optical properties of randomly inhomogeneous materials: the wavelength of the light, λ, the classical skin depth of the metal, δ, and the particle radius, a. At far-infrared frequencies our samples are in the regime where $\lambda \gg \delta > a$. In this long-wavelength limit, and at low concentrations, the far-infrared radiation induces oscillating electric and magnetic dipoles on the small metal particles. The electric dipole moment arises from the polarization of a particle in a uniform electric field, while the magnetic dipole moment arises from eddy currents induced by a time-varying, uniform magnetic field. According to classical electromagnetic theory, the imaginary part of these induced dipole moments determine the absorption of radiation. The electric dipole absorption governs the color of small-particle dispersions in the visible part of the spectrum, but it is the magnetic dipole or eddy-current absorption which dominates the theoretical far-infrared absorption.

Previous studies[1,2] of the far-infrared absorption in small metal particles found that the classical theory, while predicting the correct quadratic frequency dependence, predicted a magnitude only 0.001 to 0.1 as great as that actually observed for the absorption coefficient. In our samples, the measured absorption is about a factor of 10 larger than predicted.

Three suggestions have been advanced to account for this large discrepancy between theory and experiment. Tanner, Sievers, and Buhrman[1] proposed that quantization of the electron energy levels in small particles could change the dielectric function enough to account for the measured values; however, a subsequent reexamination of this idea by Granqvist *et al.*,[2] and Granqvist[6] concluded that this mechanism would not account for the large measured absorption.

Simanek[7] has proposed that the oxide coating on the Al small particles studied in Ref. 2 could be the absorbing medium. In his model, which has been extended by Ruppin,[8] the oxide-coated metal particles are aggregated into long cylinders, which enhance the absorption. (Electron microscopy of gas evaporated particles frequently shows that the particles have clustered into long chains.[9]) Both authors assume a value for the imaginary part of the dielectric function of the oxide coating that is relatively large. Simanek obtained a far-infrared absorption about a factor of 2 smaller than that observed by Granqvist *et al.*[2] Ruppin obtained similar results but also estimated an absorption that exceeded the experimental results of Tanner, Sievers, and Buhrman.[1] In this second case, however, the frequency dependence of the theoretical absorption was stronger than that observed experimentally.

The third theoretical treatment of this subject was by Stroud and Pan,[10] who included the effects of induced magnetic dipoles (eddy currents) and higher-order multipoles on the absorption. Although their theory predicted the correct frequency dependence of

the absorption, it predicted a magnitude about a factor of 10 smaller than that actually observed.

II. EXPERIMENTAL PROCEDURES

Our samples consisted of Pd particles randomly supported in a KCl matrix. Four factors motivated our choice of Pd and KCl: (i) The metal particles were large enough (~1-μm radius) so that their electromagnetic properties could be described by a bulk dielectric function (e.g., quantum size effects could be neglected). (ii) Palladium metal does not oxidize readily. (iii) By embedding the particles in an (almost transparent) KCl matrix, a more nearly random arrangement of metal could be obtained than possible in a powder. (iv) The volume fraction of metal in the composites could be accurately controlled.

A. Sample preparation and characterization

A composite mixture of Pd and KCl was employed in our experiments. The palladium powder, obtained from a commercial source,[11] was made by a chemical process with particular care taken to eliminate magnetic impurities. Electron microscopy of the powder showed the particles to be approximately spherical with very smooth surfaces. The average particle radius was 0.9 μm with deviations on each side of this size of about a factor of 2. A sinter made from the material[12] had a residual resistivity ratio of about 100, from which we infer a mean free path of about 1 μm.

The volume fraction of metal in each specimen was determined by separately weighing the metal and finely ground KCl powder (about 20 μm or smaller) before mixing. This mixture was poured into an evacuable die, of the type long familiar to infrared spectroscopists as the "KBr pellet press," pumped to a pressure below 10^{-3} Torr, and compressed into a solid disk-shaped pellet with a hydraulic press. The samples were then reground and repressed about five times to ensure a more random mixture. The size of these pellets was 1.4 cm in diameter and approximately 0.1 cm in thickness. (The exact thickness of a sample was chosen to give adequate transmission at the particular Pd concentration and frequency range being investigated.) Density measurements of the composite samples served as an independent check of the volume fraction of metal in the composite. Pellets pressed from pure KCl powder were clear, with a density within 0.5% that of a single crystal of KCl.

Several of the specimens were examined with a scanning electron microscope which incorporated an x-ray microprobe for elemental analysis. The x-ray technique indicated that the Pd was well distributed throughout each specimen, except for an occasional accumulation of the 0.9-μm particles into irregular blobs with typical dimension 5 μm. No evidence could be found for the long chains of particles which are known to be present in gas evaporated smokes.[9]

B. Far-infrared techniques

Two far-infrared Fourier transform spectrometers were used to make measurements between 4 cm^{-1} ($\hbar\omega \approx 0.5$ meV) and 70 cm^{-1} ($\hbar\omega \approx 9$ meV). A lamellar grating interferometer[13] covered 4 cm^{-1} to 35 cm^{-1} while a Michelson interferometer[14] was used between 25 and 70 cm^{-1}. At the measurement temperature of 4.2 K, the compressed KCl pellets were transparent below 70 cm^{-1} but absorbed quite strongly at larger wave numbers.

The far-infrared radiation traveled from the interferometer to the sample through a 1.27-cm diameter brass light pipe. The transmitted radiation was collected just below the sample and followed a light pipe through a vacuum window to a gallium-doped germanium bolometer detector operated at 1.2 K. Three composite samples and a pure KCl sample could be rotated independently into the gap between the two sections of light pipe. A fifth hole on the rotator disk was left open to measure the incident intensity.

The normal incidence transmittance of a plane parallel disk of thickness d and index of refraction $N = n + i\kappa$ is given by

$$T = \frac{(1-R)^2 \exp[-(2\omega/c)\kappa d]}{[1 - R\exp[-(2\omega/c)\kappa d]]^2 + 4R\exp[-(2\omega/c)\kappa d]\sin^2[(\omega/c)nd]} \quad . \tag{1}$$

Here R is the reflectance of either surface, given by $R = [(n-1)^2+\kappa^2]/[(n+1)^2+\kappa^2]$. The last term in the denominator of this equation gives interference oscillations, with the separation of adjacent maxima or minima given by

$$\Delta\omega = 2\pi(c/nd) \quad . \tag{2}$$

The refractive index of the specimen can be determined from the interference pattern. When the measurements are done with high enough resolution, this interference is clearly observed at frequencies where the absorption is low. When the absorption increases, however, the interference is washed out because of the attenuation of multiple internal reflections. The interference pattern can be eliminated by making low-resolution measurements. In Fourier transform spectroscopy these measurements are done by reducing the number of points in the interferogram. In this case, Eq. (1) becomes

$$T = \frac{(1-R)^2 e^{-\alpha d}}{1 - R^2 e^{-2\alpha d}} \quad , \tag{3}$$

where α is the absorption coefficient of the specimen, given by

$$\alpha = \frac{2\omega}{c}\kappa = \frac{2\omega}{c}\,\mathrm{Im}(\epsilon\mu)^{1/2} \quad . \tag{4}$$

In Eq. (4), ϵ is the complex dielectric function and μ the complex permeability of the sample. Equation (3) may be further simplified by noting that $R^2 e^{-2\alpha d} \ll 1$, so that the absorption coefficient ultimately reduces to

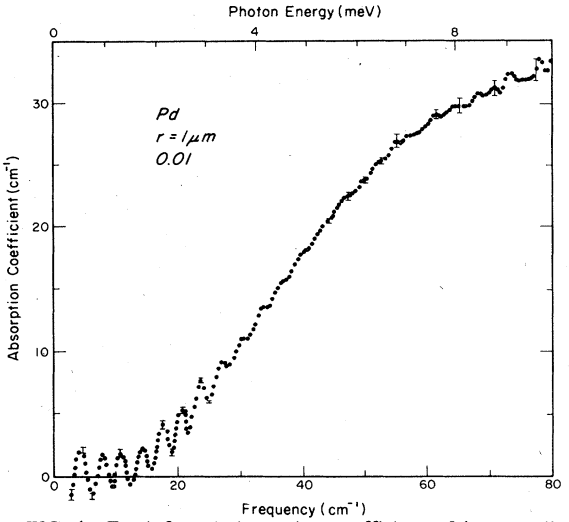

FIG. 1. Far-infrared absorption coefficient of 1-μm-radius Pd particles in KCl at a volume fraction of 0.01. The frequency resolution is 0.5 cm^{-1}. Error bars are attached to representative points.

$$\alpha = -(1/d)\ \ln(T) + \alpha_0\ , \tag{5}$$

with $\alpha_0 = (2/d)\ \ln(1-R)$. This last term is a correction for the reflectance of the sample surfaces, which we take to be independent of frequency. For KCl, $n = 2.11$ giving $R = 0.12$ and $\alpha_0 \simeq -0.25/d$. There are other corrections, of about the same magnitude, which arise from detector nonlinearities and changes of background radiation reaching the detector. Because $\alpha(\omega = 0) = 0$ for both insulators and metals, the data have been adjusted to have the absorption coefficient go to zero at the lowest frequencies.

III. EXPERIMENTAL RESULTS

The absorption coefficient of a Pd-KCl composite having a volume fraction, $f = 0.01$ is plotted in Fig. 1 with a frequency resolution of 0.5 cm^{-1}. Below 20 cm^{-1} the absorption coefficient is small with a strong interference pattern, while above 30 cm^{-1} the interference oscillations are absent. From Eq. (2), the index of refraction of this composite is $n = 2.13 \pm 0.01$, a value which is slightly larger than the refractive index of the compressed KCl: $n = 2.11 \pm 0.01$. The absorption coefficient is substantially larger at all frequencies than that reported in previous investigations[1,2] for similar values of the metal concentration. At high frequencies the absorption coefficient tends toward saturation.

In Fig. 2 the far-infrared absorption coefficient is shown for six samples. Five were composite specimens, with Pd concentrations of 0.001, 0.003, and 0.01, 0.03, and 0.1, while the sixth was a compressed KCl specimen. The data in this figure are shown in low resolution ($\Delta\omega \sim 1.5$ cm^{-1}) so that the interfer-

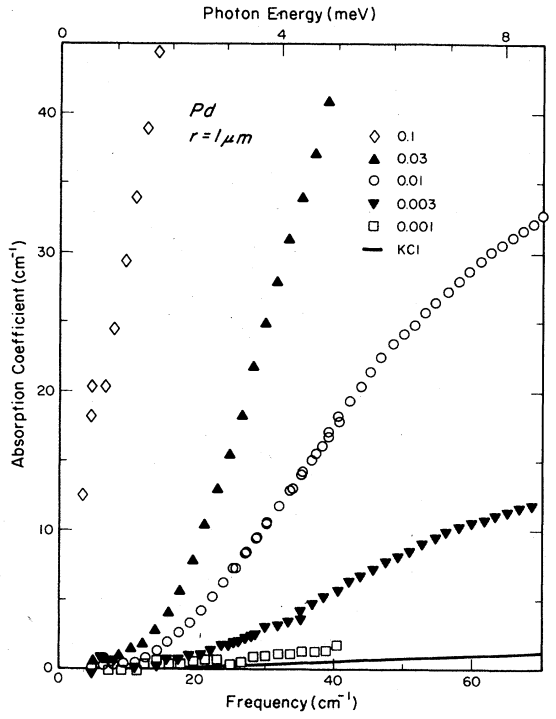

FIG. 2. Far-infrared absorption coefficient of 1-μm-radius Pd particles in KCl. Data are shown for Pd volume fractions of 0.001, 0.003, 0.01, 0.03, and 0.1, as well as for KCl itself. The frequency resolution is 1.5 cm^{-1}.

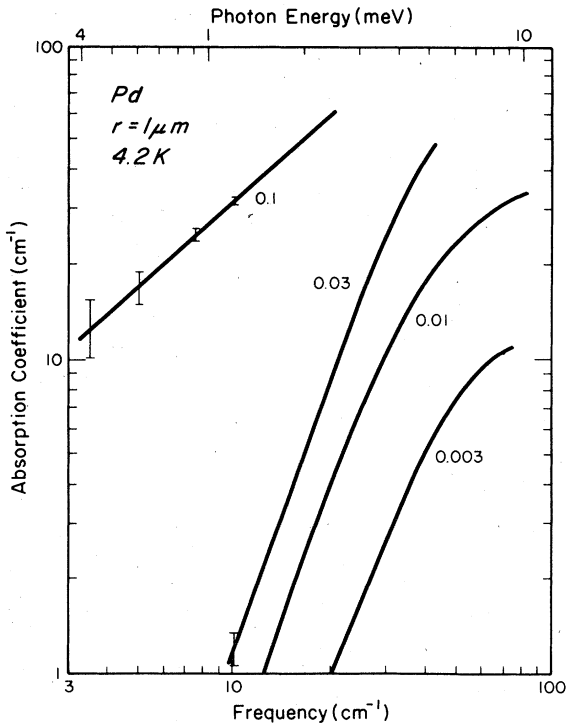

FIG. 3. Far-infrared absorption coefficient of 1-μm-radius Pd particles in KCl, shown on a log-log scale. Data are shown for Pd volume fractions of 0.001, 0.003, 0.01, 0.03, and 0.1.

ence patterns are not evident. Two sets of points are shown between 25 and 35 cm^{-1} showing the overlap between the two interferometers.

It is clear from the data that the addition of even a very small amount of Pd to the KCl substantially increases the absorption. For all samples except that having $f=0.1$, the absorption coefficient increases as $\alpha \sim \omega^2$ at low frequencies and then tends to level off. The absorption coefficient of the $f=0.1$ sample increases very rapidly at low frequencies. The power-law dependence of the absorption coefficient can be best seen in Fig. 3, in which the data are plotted logarithmically. Some caution should be used in interpreting these data because of their sensitivity to the choice of α_0 in Eq. (6). Nevertheless three of the samples, $f=0.003$, 0.01, and 0.03, show $\alpha \sim \omega^2$ below about 30 cm^{-1}. The $f=0.1$ specimen, on the other hand, has $\alpha \sim \omega$ over the range 3 to 20 cm^{-1}.

Figure 4 shows the frequency dependence of the absorption coefficient divided by volume fraction, α/f. Despite the scatter at the extremes of frequency, the specimens with $f=0.001$, 0.003, 0.01, and 0.03 follow the same curve while the $f=0.1$ sample is again qualitatively different. At 15 cm^{-1}, α/f for the $f=0.1$ sample is twice as large as it is for the other specimens. The absorption coefficient of the KCl has been subtracted from the absorption coefficient of the samples before the normalization, a correction important only in the lowest-concentration sample. The similarity of the data for the lower-concentration composites suggests that the absorption coefficient is proportional to concentration for $f \lesssim 0.03$.

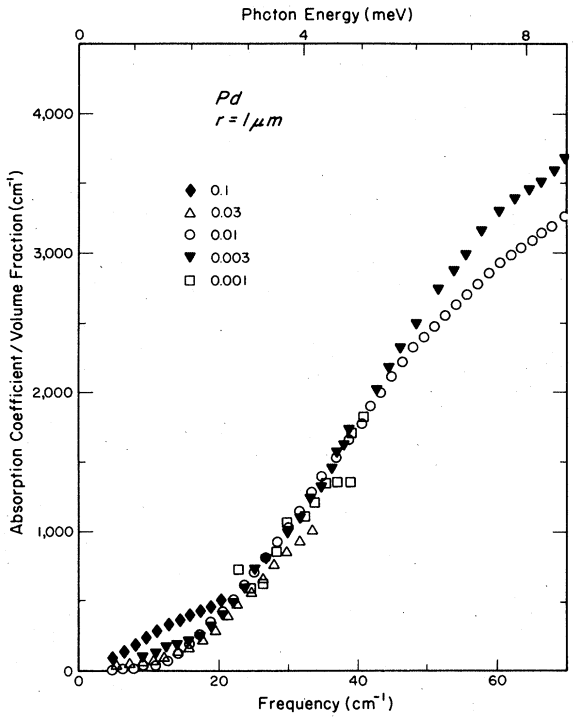

FIG. 4. Far-infrared absorption coefficient divided by the volume fraction for Pd particles in KCl. Data are shown for Pd volume fractions of 0.001, 0.003, 0.01, 0.03, and 0.1.

IV. THEORY

According to Eq. (4), the absorption coefficient which we have measured depends on the effective dielectric constant ϵ and the effective magnetic permeability μ of the composite. The calculation of the effective properties of a composite system has been the subject of theoretical interest[5–8, 10, 15–24] over many years. This calculation is done in two steps. First, the response of a single isolated particle to electromagnetic fields is found, and then an average over the behavior of a random mixture of particles is performed. Because the wavelength of the far-infrared radiation, $\lambda \geq 100$ μm, is much larger than the radius of the particle, ~ 1 μm, the fields appear to be spatially uniform at the particle so that only dipole modes enter the problem (at least at low concentrations[23, 24]). In the following paragraphs we discuss some of the factors which determine the dielectric function and magnetic permeability of the composite.

A. Dielectric function.

A particle is characterized by a complex frequency-dependent dielectric function, $\epsilon(\omega)$, which we write in terms of its real and imaginary parts as $\epsilon=\epsilon_1+(4\pi i/\omega)\sigma_1$, with $\epsilon_1(\omega)$ the real dielectric function and $\sigma_1(\omega)$ the frequency-dependent conductivity. If the particle is metallic, the dielectric function has a frequency-dependent conductivity at the lowest frequencies that is nearly equal to the dc conductivity. The imaginary part of the dielectric function is much larger than the real part. On the other hand, the dielectric function of an insulating particle has a real part which is larger than its imaginary part over most frequencies and which at the lowest frequencies is nearly equal to the static dielectric constant. In a uniform, time-dependent electric field $E=E_0e^{-i\omega t}$, the interior of a spherical particle will be uniformly polarized, while the fields outside the particle are those of an oscillating dipole.

The random mixture of particles of different properties has a dielectric function which depends on position, i.e., $\epsilon=\epsilon(\vec{r},\omega)$. Although the inhomogeneous system is completely characterized by $\epsilon(\vec{r},\omega)$, this characterization is not very useful because the interesting property is the *average* response of the system to applied fields rather than the local response. So long as the scale over which the measurement is done (the wavelength) is large compared to the distance over which $\epsilon(\vec{r},\omega)$ fluctuates (the particle size), the medium should behave as if it were homogeneous, with an effective dielectric function which depends on the dielectric functions and concentrations of each constituent but not on their particular

geometric arrangements.

Historically,[15] two different theoretical approaches have been made to this problem. The first, known as Maxwell-Garnett theory (MGT), was a molecular-field model due originally to Clausius and Mosotti and applied to optical properties by Garnett.[16] The second was a self-consistent embedding technique developed by Bruggeman[17] and studied quantitatively by Landauer.[18] The first application of this effective medium approximation (EMA) to the optical properties of inhomogeneous media was done by Stroud.[22]

In the MGT, the metal particles are considered to be randomly embedded in the insulating medium. It is further assumed that the particles do not make contact so that the theory is restricted to very dilute systems. The MGT dielectric function, ϵ_G, is defined as the ratio of volume-averaged displacement to the volume-averaged electric field and is given by

$$\epsilon_G = \epsilon_i + 3f\epsilon_i \frac{\epsilon_m - \epsilon_i}{(1-f)\epsilon_m + (2+f)\epsilon_i} , \tag{6}$$

where ϵ_i is the dielectric function of the insulating host and ϵ_m the dielectric function of the metallic inclusions. The properties of this dielectric function will be discussed after we have described the EMA approach.

In the EMA, the dielectric function of the composite ϵ_B is defined to be equal to that of a self-consistent effective medium. The self-consistency condition is that the electric field (and, therefore, the current and polarization) in the effective medium equal the average field (and current and polarization) in the inhomogeneous medium. The EMA treats each constituent of the mixture on an equal basis. A particular grain is chosen for consideration and outside this grain the material is assumed to have a homogeneous dielectric function, ϵ_B. Volume averaging the fields then gives a quadratic equation for ϵ_B:

$$f\frac{\epsilon_m - \epsilon_B}{\epsilon_m + 2\epsilon_B} + (1-f)\frac{\epsilon_i - \epsilon_B}{\epsilon_i + 2\epsilon_B} = 0 . \tag{7}$$

Of the two solutions to Eq. (7) the one with a positive imaginary part is physically significant.

At low concentrations of metal embedded in insulator ($f < 0.01$), the MGT and EMA give identical results for the far-infrared absorption in an inhomogeneous medium. Setting the dielectric function ϵ_m of the metal to have the Drude form,

$$\epsilon_m(\omega) = 1 - \omega_p^2/(\omega^2 + i\omega/\tau) \tag{8}$$

(ω_p is the plasma frequency of the metal and τ is the lifetime of the conduction electrons) and setting $\epsilon_i = 1$, the MGT dielectric function ϵ_G then reduces to the Lorentzian form

$$\epsilon_G = 1 + \frac{f\omega_p^2}{\omega_0^2 - \omega^2 - i\omega\tau} , \tag{9}$$

where the MGT resonance frequency is $\omega_0 = \omega_p\sqrt{(1-f)/3}$. The far-infrared absorption due to the electric dipole polarization in small metallic particles arises from the low-frequency tail of this resonance.

As the concentration of metal increases, the EMA predicts a metal-insulator transition at a critical volume fraction $f_c = \frac{1}{3}$. (This transition does not appear in the MGT expression.) Actual random composites generally tend to show critical volume fractions[25] in the range $0.15 \leq f_c \leq 0.20$ lower than predicted by the EMA. As the conduction threshold is approached, the EMA also predicts an increased absorption of electromagnetic radiation. Physically, this absorption results from the formation of connected clusters of metal particles which occur near the percolation threshold. It is the currents driven in these clusters by the infrared electric field which give rise to the increased absorption.

B. Magnetic permeability

A conducting particle in an alternating magnetic field $\vec{H} = \vec{H}_0 e^{-i\omega t}$ has an additional mechanism for electromagnetic absorption because of induced eddy currents. These currents circulate around the magnetic field direction and give the particle a net magnetization

$$\vec{M} = \gamma_m \vec{H}_0 , \tag{10}$$

where γ_m, the magnetic polarizability per unit volume, is[26–28]

$$\gamma_m = \frac{3}{8\pi}\frac{j_2(ka)}{j_0(ka)} , \tag{11}$$

where $k = (\omega/c)\sqrt{\epsilon}$ is the wave vector of radiation inside the particle, and

$$j_0(x) = (\sin x)/x$$

and

$$j_2(x) = (3\sin x - 3x\cos x - x^2\sin x)/x^3$$

are spherical Bessel functions. Even though the field inside the sphere is not uniform, the field outside is exactly that of a uniformly magnetized sphere whose permeability μ_m is

$$\mu_m = \frac{1 + \frac{8}{3}\pi\gamma_m}{1 - \frac{4}{3}\pi\gamma_m} . \tag{12}$$

This permeability is complex to allow for losses in the particle.

The MGT and EMA expressions for the dielectric constant of an inhomogeneous medium carry over exactly to expressions for the permeability. In the MGT the average permeability is

$$\mu_G = 1 + 3f\frac{\mu_m - 1}{(1-f)\mu_m + 2 + f} , \tag{13}$$

whereas the EMA expression for μ_B is given by the solution with positive imaginary part to

$$f\frac{\mu_m - \mu_B}{\mu_m + 2\mu_B} + (1-f)\frac{1 - \mu_B}{1 + 2\mu_B} = 0 . \tag{14}$$

In these equations μ_m is the permeability of the metal particles, while the permeability of the insulator is unity. Although the actual permeability of both me-

tallic and insulating materials is very close to unity, the permeability of the composite can be quite different from unity because of induced eddy currents.

C. Expansion at low f and low ω

At low concentrations ($f \ll f_c$) the EMA and MGT give identical results, as was mentioned above. In this limit we can expand our results at low frequencies. Using a Drude dielectric function [Eq. (8)] for the metal, $\epsilon = 1$ for the insulator and assuming that $\omega \ll 1/\tau \ll \omega_p$ (i.e., the normal skin-effect region) we find

$$\epsilon_G = 1 + 3f + i\frac{9f\omega}{\omega_p^2\tau} , \tag{15}$$

$$\mu_G = 1 - \frac{f\omega_p^2\tau^2a^2\omega^2}{10c^2} + i\frac{f\omega_p^2\tau a^2\omega}{10c^2} . \tag{16}$$

In deriving these equations, we have retained terms linear in f and of lowest order in ω. It is clear from Eqs. (15) and (16) that the polarizability of the particles enhance the dielectric constant, whereas the eddy currents give a diamagnetic susceptibility, as expected from Lenz's law.

Substituting our expressions for ϵ_G and μ_G into Eq. (4), we obtain for the absorption coefficient

$$\alpha = \frac{f\omega^2}{c^2}\left(\frac{9c}{\omega_p^2\tau} + \frac{a^2\omega_p^2\tau}{10c}\right) . \tag{17}$$

The first term in parentheses arises from the induced electric dipoles and is inversely proportional to the dc conductivity $\sigma_1(0) = \omega_p^2\tau/4\pi$, while the second term, coming from the induced magnetic dipoles, is directly proportional to the conductivity. If the conductivity is assumed to be independent of the particle radius (i.e., no boundary scattering) then the first term is independent of size while the second is proportional to the radius squared. On the other hand, if the particle size limits the mean free path to $l = v_F\tau = a$, with v_F the Fermi velocity, then the first term will be inversely proportional to radius while the second proportional to radius cubed. The contribution from the two terms are equal when $a \sim 10c/\omega_p^2\tau$ (first case) or $a \sim 3\sqrt{cv_F}/\omega_p$ (second case). For typical metals having $\omega_p = 5 \times 10^4$ cm^{-1}, $\omega_p\tau \sim 100$, and $v_F = \sim 10^8$ cm/sec, both cases predict a crossover from electric dipole to magnetic dipole absorption at a radius of 40–60 Å. For particles of larger radius, the eddy-current absorption would be expected to dominate the electric dipole absorption.

In the derivation of Eq. (17) it was assumed implicitly that $|ka| \ll 1$. This condition is equivalent to assuming that, for 1-μm particles,

$$\omega \ll c^2/a^2\omega_p^2\tau \approx 1 \text{ cm}^{-1} . \tag{18}$$

For smaller particles, having $a \approx 10^2$ Å, the condition is that $\omega \ll 10^4$ cm^{-1}. Thus for very small particles, the low-frequency expansion will be valid throughout the far infrared, while for larger particles the full expressions for ϵ and μ will produce a departure from the quadratic frequency dependence predicted by Eq. (17).

D. Calculated absorption coefficient

Figure 5 shows the far-infrared absorption coefficient calculated from Eqs. (4), (6), (11), (12), and (13). The volume fraction of metal for all three curves was $f = 0.01$, the particle radius was $r = 1$ μm, and the dielectric function of the insulator was $\epsilon_I = 4.8$. A Drude dielectric function, Eq. (8), was used to describe the Pd, with $\omega_p = 6$ eV (5×10^4 cm^{-1}), a value that we have inferred from the measurements of Weaver.[29] The three curves correspond to different values of the relaxation time τ. For the solid line, τ was chosen to give a dc conductivity equal to the room-temperature value for Pd ($\sigma = 8 \times 10^5$ Ω^{-1} cm^{-1}, $1/\tau = 500$ cm^{-1}). For the dashed line the conductivity was 10 times the room-temperature value ($1/\tau = 50$ cm^{-1}) while for the dotted line the conductivity was 100 times the room-temperature value ($1/\tau = 5$ cm^{-1}).

The shape of the calculated absorption coefficient for $\sigma/\sigma_{Pd} = 1$ shown in Fig. 5 is qualitatively similar to the experimental curve for $f = 0.01$ in Fig. 2. In each case, the absorption coefficient increases quadratically with frequency at the lowest frequencies and tends to level off at higher frequencies. The saturation at high frequencies is a consequence of the skin depth in the Pd particles becoming smaller than the particle radius. In this skin-effect regime, the interior of the particles is screened from the electromagnetic fields.

Although the shapes of the experimental and

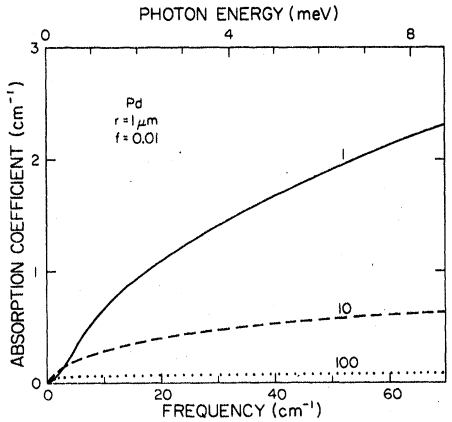

FIG. 5. Calculated far-infrared absorption coefficient (using either the EMA or the MGT). The calculations were done for 1-μm-radius particles in KCl at a volume fraction of 0.01 using Drude parameters appropriate to Pd. The three curves shown are for three values of these parameters, corresponding to dc conductivities equal to the room-temperature value (solid line), 10 times (dashed line), and 100 times (dotted line) the room-temperature value.

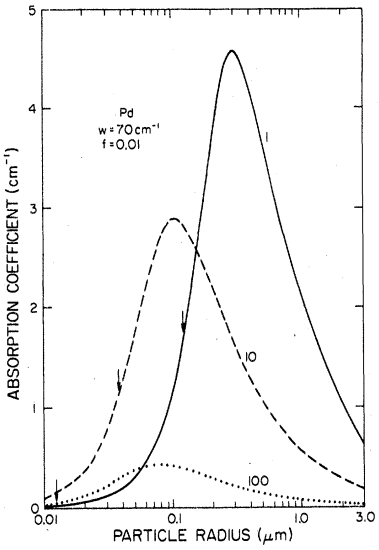

FIG. 6. Calculated absorption coefficient for volume fraction 0.01 at 70 cm^{-1} (using either the EMA or the MGT) vs particle radius. The three curves shown are for dc conductivity of the metal equal to 1 (solid line), 10 (dashed line), and 100 (dotted line) times the room-temperature conductivity of Pd. The arrows indicate the size for which the skin depth equals the radius.

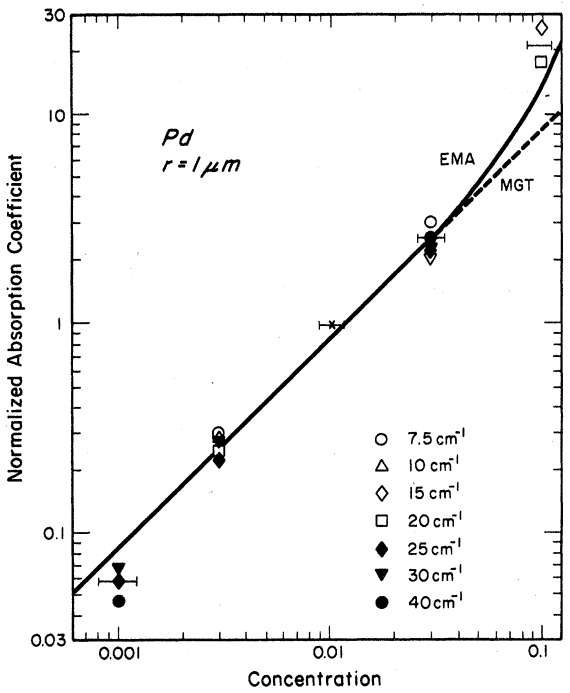

FIG. 7. Normalized absorption coefficient of 1-μm-radius Pd particles in KCl vs concentration. The data for the $f=0.001$, 0.003, 0.03, and 0.1 volume fraction samples have been divided by the data for the $f=0.01$ volume fraction sample.

theoretical curves are in agreement, the magnitude of the calculated absorption is smaller than the measured value by about a factor of 10. At $\omega=70$ cm^{-1}, the theoretical absorption coefficient is $\alpha=2.3$ cm^{-1} while the experimental coefficient is $\alpha=33$ cm^{-1}. The agreement is somewhat better at low frequencies. For example, at $\omega=20$ cm^{-1}, the theory gives $\alpha=1.2$ cm^{-1} while the experiment gives $\alpha=3$ cm^{-1}.

The dependence of the absorption coefficient on particle radius is shown in Fig. 6, for a frequency of 70 cm^{-1}. The arrows on each curve indicate the value of the classical skin depth $\delta=c/\sqrt{2\pi\sigma_0\omega}$. As the particle radius increases, the absorption is seen to increase rapidly to a maximum value at a radius two to five times larger than the skin depth. At larger radii, the absorption coefficient decreases because the fields penetrate into the particle a progressively shorter distance. The absorption maximum, $\alpha=4.6$ cm^{-1} at $r=0.3$ μm is still nearly a factor of 10 smaller than the experimental value. It is not possible to improve substantially the agreement by adjusting the assumed conductivity of the metal particles.

V. DISCUSSION

In the work described above, we have investigated the far-infrared absorption in random small particle composites. The metal small particles were 100 times larger in diameter than those studied previously[1,2]; furthermore, the metal particles in this study were supported in an insulating host. These differences mean that the metal could be described by its bulk dielectric function (size effects being unimportant) and that a random mixture of metal and insulator could be obtained (as assumed by the theories).

There are two main areas of agreement between our data and our calculations. First, the frequency dependence of the theory is in good agreement with experiment; the absorption coefficient is quadratic in frequency at low frequencies, while at higher frequencies the absorption coefficient tends to saturate. This saturation is believed to result from the skin-effect screening of the applied far-infrared radiation at the surface of each metal particle.

The second area of agreement is the concentration dependence of the absorption coefficient. Figure 7 shows the normalized absorption coefficient of our samples versus metal volume fraction. This normalized absorption coefficient is the ratio of the absorption coefficient at a particular frequency to the value of the absorption coefficient of the $f=0.01$ sample at that frequency. The two curves shown are calculated from the EMA and the MGT. The MGT predicts a linear increase in absorption coefficient with metal volume fraction over the entire concentration range. The EMA is linear at low concentrations but predicts a faster increase in absorption at concentrations between a few percent and the percolation transition. This rise is a precursor of the very large absorption

coefficient of conducting composites. Our data are in reasonable accord with the EMA for all concentrations.

Although successful in explaining the frequency and concentration dependence of the absorption coefficient, classical electromagnetic theory fails to explain the magnitude of the far-infrared absorption. The magnitude of the absorption coefficient in our samples is about ten times larger than can be calculated using reasonable values in the equation of Sec. IV.

To explain the magnitude of the absorption in very small Al particles,[2] Simanek[7] has proposed that the absorption occurs in an oxide coating on the surface of the particles. The effect of oxide layers or adsorbed molecules on the surface of our particles would be expected to be relatively small because their large size (compared to those previously studied) reduces their surface-to-volume ratio. If in Simanek's theory we use particle radii of 1 μm and his assumed values for an oxide coating [thickness 30 Å and dielectric function $\epsilon = 10 + i(3.8 \times 10^{-3})\omega$ with ω in cm^{-1}] we estimate a maximum absorption at 70 cm^{-1} of $\alpha = 1.6$ cm^{-1}, considerably smaller than observed. Thus we cannot explain the magnitude of the absorption in our samples by ascribing it to an oxide coating.

We believe the magnitude of the absorption anomaly lies in the clustering of particles. It is well known from percolation theory that small clusters of connected particles form in any randomly inhomogeneous system. The size of these clusters grows with increasing metal volume fraction, eventually becoming infinite at the percolation transition. If there are interactions among particles, either through tunneling across an oxide barrier or through direct electrical contact, and if these interactions are not strong enough to screen the applied radiation from the interior of the cluster, then the absorption would be increased above the isolated-grain values calculated in Sec. II. The importance of clustering in enhancing the absorption in oxide coatings was stressed by Simanek[7] and by Ruppin.[8] This clustering effect will obviously be most important in random composites as the percolation threshold is approached.

ACKNOWLEDGMENTS

The authors are grateful for many useful conversations with D. Stroud, D. M. Grannan, W. J. Lamb, and R. L. Henry, and for assistance with KCl density measurements by B. Warner. This research was supported by the U.S. DOE through Contract No. DE-AS02-78ER04914.

[1]D. B. Tanner, A. J. Sievers, and R. A. Buhrman, Phys. Rev. B 11, 1330 (1975).
[2]C. G. Granqvist, R. A. Buhrman, J. Wyns, and A. J. Sievers, Phys. Rev. Lett. 37, 625 (1976).
[3]L. P. Gor'kov and G. M. Eliashberg, Sov. Phys. JETP 21, 940 (1965).
[4]N. E. Russell, G. L. Carr and D. B. Tanner, in *Electrical Transport and Optical Properties of Inhomogeneous Media,* edited by J. C. Garland and D. B. Tanner (AIP, New York, 1978), p. 263.
[5]*Electrical Transport and Optical Properties of Inhomogeneous Media,* edited by J. C. Garland and D. B. Tanner (AIP, New York, 1978).
[6]C. G. Granqvist, Z. Phys. B 30, 29 (1978).
[7]E. Simanek, Phys. Rev. Lett. 38, 1161 (1977).
[8]R. Ruppin, Phys. Rev. B 19, 1318 (1979).
[9]C. G. Granqvist and R. A. Buhrman, J. Appl. Phys. 47, 2200 (1976).
[10]D. Stroud and F. P. Pan, Phys. Rev. B 17, 1602 (1978).
[11]Leico Industries, New York, N.Y.
[12]K. A. Muething, Ph.D. thesis (The Ohio State University, 1979) (unpublished).
[13]R. L. Henry and D. B. Tanner, Infrared Phys. 19, 163 (1979).
[14]R. B. Sanderson and H. E. Scott, Appl. Opt. 10, 1097 (1971).
[15]A complete historical review of this subject is given by Rolf Landauer, in *Electrical Transport and Optical Properties of Inhomogeneous Media,* edited by J. C. Garland and D. B. Tanner (AIP, New York, 1978), p. 2.
[16]J. C. Maxwell Garnett, Philos. Trans. R. Soc. London 203, 385 (1904); 205, 237 (1906).
[17]D. A. G. Bruggeman, Ann. Phys. (Leipzig) 24, 636 (1935).
[18]R. Landauer, J. Appl. Phys. 23, 779 (1952).
[19]L. Genzel and T. P. Martin, Phys. Status Solidi (b) 51, 91 (1972); Surf. Sci. 34, 33 (1973).
[20]A. S. Barker, Jr., Phys. Rev. B 7, 2507 (1973).
[21]R. W. Cohen, G. D. Cody, M. D. Coutts, and B. Abeles, Phys. Rev. B 8, 3698 (1973).
[22]D. Stroud, Phys. Rev. B 12, 3368 (1975); 19, 1783 (1979).
[23]R. C. McPhedran and D. R. McKenzie, in *Electrical Transport and Optical Properties of Inhomogeneous Media,* edited by J. C. Garland and D. B. Tanner (AIP, New York, 1978), p. 294.
[24]W. T. Doyle, in Ref. 23, p. 300.
[25]J. C. Garland, W. F. Gully, and D. B. Tanner, Phys. Rev. B 22, 507 (1980); D.M. Grannan, J. C. Garland, and D. B. Tanner (unpublished).
[26]L. D. Landau and E. M. Lifshitz, *Electrodynamics of Continuous Media* (Pergamon, New York, 1960), Secs. 72 and 73.
[27]G. W. Ford and S. A. Werner, Phys. Rev. B 8, 3702 (1973).
[28]We have ignored the nonlocal aspects of the eddy-current problem in our calculations. These effects have been discussed by H. J. Trodahl, Phys. Rev. B 19, 1316 (1979). In our relatively large particles, the electron mean free path may be shorter than the particle diameter. A sufficiently short mean free path would eliminate these nonlocal effects. Trodahl finds that the nonlocal effects *reduce* the far-infrared absorption resulting from eddy currents by a factor of $\frac{5}{8}$.
[29]J. H. Weaver, Phys. Rev. B 11, 1416 (1975).